Journal of Hydrology 575 (2019) 343–353

Contents lists available at ScienceDirect

Journal of Hydrology

journal homepage: www.elsevier.com/locate/jhydrol

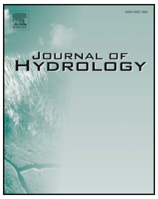

Research papers

Water balance and tree water use dynamics in remnant urban reserves

V. Marchionni[a,*], A. Guyot[a], N. Tapper[b], J.P. Walker[a], E. Daly[a]

[a] *Department of Civil Engineering, Monash University, Melbourne, Australia*
[b] *School of Earth, Atmosphere, and Environment, Monash University, Melbourne, Australia*

ARTICLE INFO

This manuscript was handled by Marco Borga, Editor-in-Chief

2010 MSC:
00-01
99-00

Keywords:
Groundwater dependent ecosystems
Remnant vegetation
Urban green spaces
Urban parks
Urban reserves
Heat stress

ABSTRACT

During the expansion of urban areas, small natural reserves have often been left intact within the built environment as central elements of biodiversity conservation, ecological connectivity, landscape sustainability, and quality of life of urban dwellers. Consequently, the surrounding urbanized landscape may impact the environmental conditions of these reserves (e.g., high temperatures, low moisture conditions), resulting in the need for extensive maintenance. This study presents an estimation of the water balance over two years (2017–2018) in three small urban reserves (between 2 and 30 ha) within the Greater Melbourne metropolitan area in Australia, for the purpose of understanding tree water use. Measurements of micrometeorological variables, soil moisture content profiles, water-table levels, sap flow velocities, and stem diameter variations were used to quantify the water sources of tree transpiration in these reserves. Results revealed that, despite the urban surroundings and the climate variations, these reserves have enough water to sustain tree transpiration. In two of the three reserves, groundwater was pivotal in sustaining transpiration rates; specifically, groundwater was estimated to contribute about 30–40% of the total transpiration amount during the driest periods of the year. Groundwater also played an essential role during nights with temperatures above 25 °C, helping trees to maintain night-time water use from 3 to 16% of the daily water use. In the third reserve, the presence of a shallow layer of heavy clay supplied water to the trees, which were able to maintain relatively constant transpiration rates throughout the year. These results demonstrate the importance of understanding the water regime of each urban reserve in order to support government authorities in preserving these ecosystems.

1. Introduction

The rapid expansion of urban areas to accommodate the growing number of city dwellers represents one of the most irreversible human impacts on the global biosphere and poses unique challenges for ecosystems (Seto et al., 2012). Changes in land cover associated with urbanization generate a fragmented and heterogeneous landscape where patches of vegetation, often remnants of natural habitats, are embedded in a highly disturbed environment (McKinney, 2002). Remaining pockets of vegetation within the built environment are recognized as important areas for biodiversity conservation (Elmqvist et al., 2015; Tulloch et al., 2016; Melaas et al., 2016; Lepczyk et al., 2017), mitigating the urban heat island (UHI) effect (e.g., Bowler et al., 2010; Gill et al., 2007; Declet-Barreto et al., 2016), and restoring hydrological and biogeochemical processes closer to natural conditions (e.g., Yang et al., 2015; Livesley et al., 2016; Berland et al., 2017).

Considering its importance, there are concerns that the urban surrounds may be exerting negative impacts on the remaining vegetation, by imposing changes in the radiation and energy budget, the hydrologic regime, and ecosystem composition and structure (Roberts, 1977; Sieghardt et al., 2005). Specifically, increased temperatures and lower air humidity due to the UHI often expose the trees embedded in the urban landscape to high atmospheric evaporative demand. This can lead to higher transpiration rates, in particular when soil moisture is not a limiting factor (Litvak et al., 2011; Chen et al., 2011; Litvak and Pataki, 2016; Zipper et al., 2017; Litvak et al., 2017; Asawa et al., 2017).

The increase of impervious surfaces and the introduction of drainage infrastructure lead to greater rates and volumes of surface runoff, and reduce the volume of water which infiltrates the soils, decreasing the water available to sustain vegetation growth and health (Xiao et al., 2007; Barron et al., 2013; Shields and Tague, 2015). In addition, increasing drought (Van Loon et al., 2016) and extreme heat events amplify the water stress of urban trees, resulting in the decline of their health conditions. During heat events, being photosynthesis and stomatal conductance strongly coupled, net rates of leaf photosynthesis and transpiration are expected to decline toward zero due to the high temperatures and vapor pressure deficit (VPD). Recent studies,

---

* Corresponding author.
E-mail address: valentina.marchionni@monash.edu (V. Marchionni).

https://doi.org/10.1016/j.jhydrol.2019.05.022
Received 2 October 2018; Received in revised form 3 May 2019; Accepted 6 May 2019

however, found that cooling of leaves by transpiration might be an important component to plant response to extreme temperatures, leading to substantial rates of transpiration (Drake et al., 2018).

What remains of natural habitats within urban areas can also undergo changes in vegetation structure with the introduction of non-native species, thus creating unique biotic communities with different water needs and more complex patterns of evapotranspiration, interception, and infiltration (Endter-Wada et al., 2008; McCarthy and Pataki, 2010; Pataki et al., 2011). In the Greater Melbourne metropolitan area (Australia), for instance, large areas of native vegetation have been replaced by urban and suburban landscapes over the past decades (DELWP, 2016). The consequences for the native plants are substantial, with less than 4% cover of native vegetation remaining within the urban growth boundary (Bradshaw, 2012; Hahs and McDonnell, 2014). This remaining native vegetation is severely fragmented into small reserves, which become isolated and sometimes degraded. Moreover, a further decline in vegetation health have been documented during the Millennium Drought that occurred approximately between 2001 and 2009 (van Dijk et al., 2013).

In this context, maximizing the effectiveness of remnant native vegetation conservation through active management is important to avoid further losses of vegetation associated with urbanization. Therefore, there is an increasing need for empirical evidence of the role that water availability and the built landscape play in the physiological response of vegetation to urban conditions (Livesley et al., 2016). More information is also needed to understand the water requirements of these green spaces, enabling better design management guidelines for the preservation of these ecosystems. This involves the identification of the water resources that are most important to maintain key ecosystem features and processes, including the degree of the ecosystem groundwater dependency (Eamus and Froend, 2006; O'Grady et al., 2006).

This study aims to gain a better understanding of the interactions and feedback between water resources and vegetation health in small natural reserves embedded in the urban environment. The objectives are to: (a) determine variations in the water balance of urban reserves under different water regimes, (b) analyze the influence of micro-meteorological drivers and groundwater availability on tree water use, and (c) understand the impact of heat stress on night-time tree water use.

2. Material and methods

2.1. Study sites

This study was conducted in the Greater Melbourne metropolitan area, located in southeast Australia. Melbourne has a maritime/temperate climate (Köppen climate classification Cfa), with a strong spatial heterogeneity of rainfall within the metropolitan area, decreasing from south-east to north-west. The study focused on three urban reserves hosting predominantly remnant native vegetation with occasionally introduced species: National Drive Reserve and Alex Wilkie Reserve are embedded in the south-eastern suburbs, while Napier Park is located about 9 km north-west of the Melbourne Central Business District (CBD) (Fig. 1a).

National Drive Reserve (ND) covers an area of 14 ha and is located about 40 km from the Melbourne CBD. The area consists of a large stand of *Eucalyptus Camaldulensis* (River Red Gum) woodland with the understory dominated by pasture grasses. The soil is predominantly silty clay in the first 40 cm followed by clay, with the water table depth ranging between 3 and 4 m below the ground surface. Long-term average annual rainfall is 757 ± 148 mm (mean ± SD), mean minimum temperature is 10.0 °C and mean maximum temperature is 19.8 °C (1968–2018, Bureau of Meteorology (BOM), station 086224; the station 086077 located at about 10 km from ND was also used to fill extensive data gaps in daily temperature series).

Alex Wilkie Nature Reserve (AW) is a sandy plain woodland of about 1.8 ha located 10 km to the north-west of National Drive Reserve. The reserve is populated mostly with *E. Viminalis* (Coast Manna Gum) and *E. Cephalocarpa* (Silver-leafed Stringybark), with other natural and planted lower trees (e.g., *Allocasuarina Littoralis*, *Banksia Marginata*) and shrubs. The soil consists of loamy sand, which becomes sandy clay to about 3 m below ground level and then silty sand at about 7 m below ground level. The depth to groundwater ranges between 3 and 5 m below the ground surface. Long-term average annual rainfall is 684 ± 132 mm, mean minimum temperature is 10.2°C, and mean maximum temperature is 19.8 °C (1968–2018; BOM, station 086077).

Napier Park (NP) (4.1 ha) is home to a valuable population of *E. Camaldulensis* with a number of significant *E. Melliodora* (Yellow Box). Texture-contrast soils (duplex) cover the entire area of the reserve, with the soil profile consisting of a sandy silt (up to 0.6 m), overlaying a heavy clay (between 0.6 and 1.8 m) followed by sandy silt again. Groundwater depth is about 20 m below the ground surface. Long-term average annual rainfall is 557 ± 119 mm, mean minimum temperature is 10.0 °C, and mean maximum temperature is 20.4 °C (1968–2018; BOM, station 086038). Concerns over declining ecological condition of the existing remnant vegetation led to the installation of an extensive irrigation system utilizing stormwater harvesting; irrigation commenced in January 2016. Water delivery aims to recharge the soil stores for about 85% of the reserve, responding to the site specific requirements of the remnant population of *E. Camaldulensis*, which needs to be intermittently flooded.

2.2. Stand characteristics

The study was conducted over the two-year period from July 2016 to June 2018. Several 50 m × 50 m plots were selected in each reserve covering a range of vegetation and environmental conditions (e.g., moisture conditions) (Fig. 1). Stand density (stems ha^{-1}) for each plot was calculated from tree count and area, taking into account both live and dead trees. Total basal area (BA, m^2ha^{-1}) was estimated by measuring diameter at breast height (DBH, at 1.3 m from the ground) of all trees (alive and dead) with stems larger than 10 cm in diameter, including multi-stemmed trees. Percentage of live basal area (%LBA) was then calculated as the proportion of the total basal area contributed by live trees.

2.3. Micrometeorology

Micrometeorological data, including rainfall (P), air temperature (T_a), relative humidity (RH), and incoming shortwave solar radiation (R_s) were measured every 15 minutes using automatic weather stations (AWS) (Campbell Scientific). Daily vapor pressure deficit (VPD) was calculated from T_a and RH. Measurements were conducted in appropriate open grassy areas within ND and AW reserves for the entire period of the study; at NP, a weather station was placed within a private garden adjacent to the park between November 2016 to February 2017.

The data collected from the site specific weather stations were combined with the data from the closest BOM weather stations (i.e., BOM stations: 086224 for ND, 086077 for AW, and 086038 for NP) to estimate long-term (1968–2018) average annual rainfall and temperature for all sites, to fill data gaps in the rainfall time series recorded at ND (between July to December 2016) and AW (in March and July 2017 as well as from September 2017 to June 2018), and to integrate the limited time series of micrometeorological data available from the AWS installed at NP (i.e., from November 2016 to February 2017).

Comparing the BOM data with the data recorded at ND, AW, and NP using AWS, a good agreement was found in terms of monthly rainfall for ND (R^2 0.84), and in terms of weekly and monthly rainfall for AW (R^2 0.86 and 0.94, respectively) and NP (R^2 0.74 and 0.81, respectively); therefore, BOM data were used to fill gaps in the data collected from the site specific weather stations.

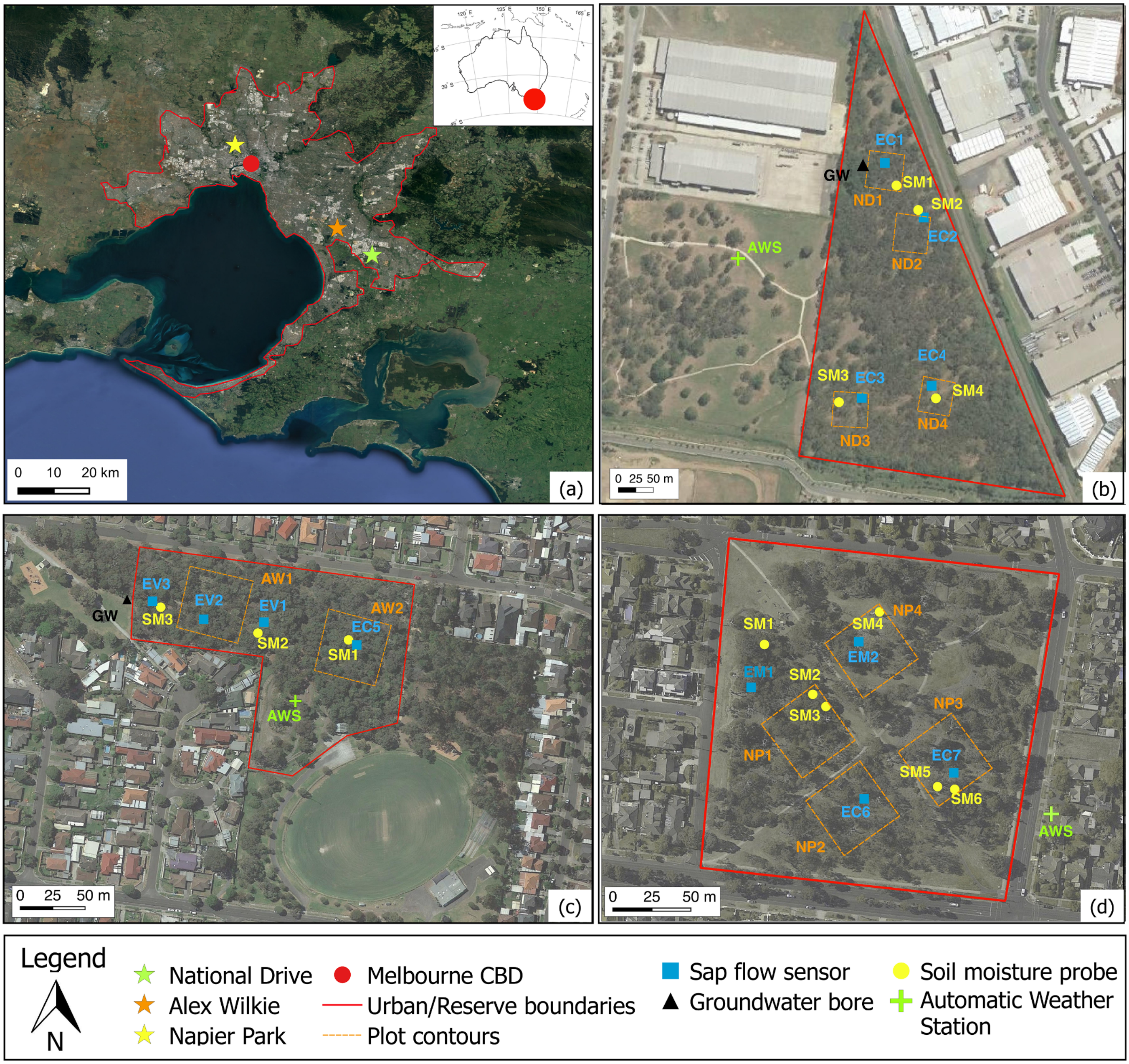

Fig. 1. (a) Location map of the experimental plots and equipment for (b) National Drive Reserve (ND), (c) Alex Wilkie Nature Reserve (AW), and (d) Napier Park (NP).

2.4. Soil water and groundwater

Soil volumetric water content (θ) and soil temperature were measured every 15 minutes using fully encapsulated soil water capacitance probes (Drill & Drop, Sentek). These probes measure the volumetric water content through sensors fixed at 10 cm increments from the surface to a depth of 120 cm. Five probes were installed at ND, three at AW, and six at NP. Measurements were validated using the gravimetric method with oven drying (O'Kelly, 2004), which involves the collection, using a sampling ring, of soil samples around the probes at different measuring depths. In our specific case, soil samples were collected at 5 cm and 15 cm depths, as deeper soil layers could not be reached due to the nature of the soils at all sites. The samples were then used to estimate dry mass and bulk density (i.e., dry mass of the soil in the given sampling volume), the latter showing variations with depth ($\rho_{bulk,5cm} = 1.1 \pm 0.2\,\mathrm{g/cm^3}$;$\rho_{bulk,15cm} = 1.4 \pm 0.1\,\mathrm{g/cm^3}$). Good agreement was found between θ measured with the Drill & Drop sensors and that estimated from the volumetric soil sample analysis in the first 20 cm of soil.

Water-table depth (relative to the ground surface) was measured at 15-min intervals in monitoring bores at ND (11.1 m depth) and AW (9 m depth). Each bore was equipped with a water level datalogger (3001 LT Levelogger Edge, Solinist) and a barometric datalogger (3001 LT Barologger Edge, Solinist) to enable specific barometric compensation. Manual water level measurements were conducted on a regular basis using a dip meter (dipper-T, Heron Instrument Inc.) to validate the water level measurements.

Uncertainties related to the measurements of θ in the top 1.2 m of

Table 1
Plot characteristics at the three study sites.

Plot[a] Code	DBH[b] (m)	Stand density (stems ha^{-1})	BA[b] (m^2 ha^{-1})	N. Trees Alive (LBA[b], %)	Monitored Trees[c] (DBH, m)
ND1	0.31 ± 0.12	632	41.2	109 (91)	EC1[d] (0.36)
ND2	0.32 ± 0.14	404	33.2	84 (95)	EC2 (0.33)
ND3	0.40 ± 0.13	248	27.6	47 (95)	EC3[d] (0.29)
ND4	0.24 ± 0.13	704	38.9	157 (96)	EC4[d] (0.29)
AW1	0.19 ± 0.09	600	23.8	116 (66)	EV3[d] (0.21), EV4 (0.21)
AW2	0.22 ± 0.10	428	18.4	93 (91)	EV1[d] (0.31), EC5 (0.46)
NP1	0.16 ± 0.09	336	18.0	62 (35)	EM1 (0.28)
NP2	0.24 ± 0.24	148	19.8	32 (58)	EC6 (0.22)
NP3	0.24 ± 0.19	128	19.8	29 (76)	EC7[d] (0.22)
NP4	0.19 ± 0.16	256	18.7	37 (38)	EM2 (0.19)

[a] ND: National Drive Reserve, AW: Alex Wilkie Reserve, NP: Napier Park.

[b] DBH: Diameter at Breast Height; BA: Basal Area; LBA: Live Basal Area.

[c] Identification of the trees equipped with sap flow sensors in each plot (Fig. 1); EC: *Eucalyptus Camaldulensis*, EV: *Eucalyptus Viminalis* EM: *Eucalyptus Melliodora*.

[d] Trees equipped with band dendrometers.

soil (i.e., ±0.03%) and water-table depths (i.e., ±0.05%) were not considered in the water balance, as annual changes in θ and water-table depths were small compared to the other components of the water balance.

2.5. Sap flow measurements and stand transpiration

Water use of individual trees was determined using commercially available sap flow sensors (SFM1, ICT International, Australia), which use the heat pulse velocity (HPV) technique to measure high, low, and reverse rates of sap flow from the velocity of a short pulse of heat moving along the xylem tissue. HPV was recorded at half-hourly intervals in several trees within the reserves and corrected for wounding effects following Burgess et al., 2001; wound widths were obtained from data in the literature collected for similar trees. Sensors were placed approximately at breast height (1.30 m from the ground) on a total of twelve trees, four at each site (Table 1). Because the reserves are open to the public, the number of trees selected could not be larger and remain inconspicuous. Measurements were converted to sap flux density (SFD, $cm^3 cm^{-2} h^{-1}$), based on wood core measurements of dry wood density, gravimetric sapwood moisture content, and sapwood area (calculated from stem diameter and thickness of sapwood and bark).

During warm summer nights with temperatures above 25 °C (and consequent high VPD; Forster, 2014), the magnitude of night-time SFD (SFD_n) was estimated as a proportion of the 24-h sap flow, considering SFD_n from 23:00 to 05:00, following the method proposed by Zeppel et al., 2010.

Plot-level transpiration (T_{plot}) was calculated from the water use of individual trees using the linear relationship ($R^2 = 0.86$, $p < 0.05$) between DBH (cm) and sapwood area ($A_{sapwood}$, cm^2) established based on the twelve selected trees across the three study sites (Fig. 2). Estimates of T_{plot} ($mm\,h^{-1}$) were thus calculated as:

$$T_{plot} = \frac{SFD_{avg} A_T}{A_{plot} \cdot 10^4}, \tag{1}$$

$$A_T = \sum_{i=1}^{N} (10.02 \cdot DBH_i - 91.90), \tag{2}$$

where A_T is the total sapwood area in a plot (cm^2), SFD_{avg} is the average area-weighted SFD ($mm\,h^{-1}$) of the measured trees in the plot, and N is the number of trees within the 50 m × 50 m plot area A_{plot} (m^2). The transpiration at the scale of the reserve (T) was estimated by averaging T_{plot} for all measurement plots within each study site.

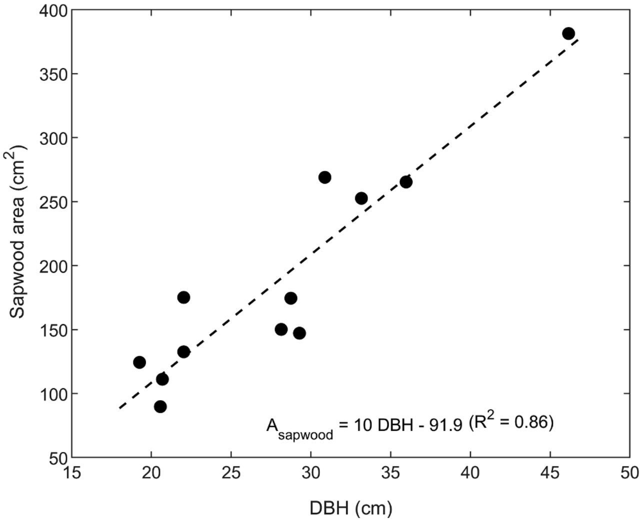

Fig. 2. Relationship between tree diameter at breast height (DBH) and sapwood area ($A_{sapwood}$).

Potential errors in the measurements of SFD using HPV sensors might lead to an underestimation of the actual SFD of up to 35% after wound correction. These errors increase with SFD and are mainly caused by heterogeneity of the sapwood (Steppe et al., 2010). Additional errors may occur during the scaling of measurements from a single point to the whole tree due to the radial and circumferential variability in sap flux density; the magnitude of this error mainly depends on the width of the sapwood area (Nadezhdina et al., 2002). The HPV technique is recognized to be the most accurate when compared to the thermal dissipation (Peters et al., 2018) and heat field deformation methods. Estimates of transpiration from stem sap flow data should also include a lag coefficient to account for the withdrawal of water from internal storage. Several studies demonstrated that 10 to 15% of daily transpiration may be provided by stem water stores (e.g., Meinzer et al., 2004; Matheny et al., 2015). However, because the dynamics of stored water affect mainly the patterns of intra-daily transpiration (Matheny et al., 2015), they have not been taken into account in this study.

2.6. Stem diameter variation measurements

A total of six trees among the ones monitored with sap flow sensors were also equipped with band dendrometers (DBL60, ICT International, Australia), to measure tree diameters over time (Table 1). The DBL60 sensors were fixed to the tree trunk with a 12 mm wide stainless steel tape at about 1.3 m height on the southern side of the tree. A portion of the outermost bark was removed prior to installation to provide an undisturbed point of contact for the tape. Stem diameter variation (SDV) and temperature were recorded every 5 minutes; SDV signals were then corrected for sensor temperature sensitivity, applying an average thermal expansion coefficient of $1.17 \cdot 10^{-6} \mu m\, (\mu m °C)^{-1}$ according to Vandegehuchte et al., 2014.

2.7. Water balance

An estimation of the water balance of each reserve was conducted out for 2 years (July 2016 to June 2017, referred to as 2017 water year, and July 2017 to June 2018, referred to as 2018 water year) using:

$$P - T - \Delta S = Q + ET + \epsilon, \tag{3}$$

where P is rainfall, T is tree transpiration ($T = T_{sw} + T_{gw}$), T_{sw} and T_{gw} are the transpiration components depleting the unsaturated and saturated zones, respectively, ΔS is total water storage change ($\Delta S = \Delta S_{sw,s} + \Delta S_{sw,d} + \Delta S_{gw}$), accounting for unsaturated soil water change in the first 1.2 m of monitored soil ($\Delta S_{sw,s}$), unsaturated deep soil water change (below 1.2 m) 1.2 m) ($\Delta S_{sw,d}$), and unconfined groundwater storage change (ΔS_{gw}), Q is runoff, ET is evapotranspiration ($ET = ET_{floor} + E_i$), accounting for floor evapotranspiration (ET_{floor}), including grass, ferns, and small shrubs, and canopy interception (E_i), and ϵ is the water balance errors including systematic errors in the estimates of the water budget variables. All terms of Eq. (3) are expressed in equivalent water depths per unit of ground area (mm). The equation was used to estimate $ET + \Delta S_{sw,d} + \epsilon$ for each site on a water year basis, Q being negligible in all study sites.

The change in soil water storage ($\Delta S_{sw,s}$) was calculated as the average change in volumetric water content in the soil profile at each measurement point (i.e., the average water content for the 12 sensors over the length of the probe). The change in groundwater storage (ΔS_{gw}) was calculated only for ND and AW reserves as the change in water table depth between consecutive years multiplied by the specific yield. The specific yield was estimated as a function of the sediment texture, as recommended for depths to the water table greater than 1 m (Loheide et al., 2005); in particular, the specific yield at ND was estimated as 2% and 7% at AW, as in Johnson, 1963.

Deeper roots also extend below the depth to which soil water probes were installed, reaching the water table or its capillary fringe. To quantify the groundwater uptake (T_{gw}) by trees in the sites where plants have access to groundwater, the method developed by White (White, 1932), and later refined by Loheide et al., 2005, was used. Accordingly,

$$T_{gw} = S_y(24r \pm s), \tag{4}$$

where S_y (–) is the specific yield, r (mm h^{-1}) is the rate of water table rise from midnight to 4 a.m., and s (mm) is the rise or fall of the groundwater level over a 24 h period (i.e., from midnight to midnight). The method was applied during rain-free periods of few days, for which water levels in the bores during the night can be reasonably assumed to be due to a net recovery flux toward the bore (Orellana et al., 2012).

3. Results

3.1. Stand characteristics

Stand characteristics differed significantly across reserves, as well as between plots within the same reserve (Table 1). ND was overall the more dense site (248–704 stems ha^{-1}) with a woodland structure that varied from east to west across the reserve. Higher basal area was found in plots ND1 (ca. 41 m^2 ha^{-1}) and ND4 (39 m^2 ha^{-1}) in the north-east and south-east parts of the site, respectively. In all plots, living trees accounted for more than 90% of the total basal area with a size about 2.2 times larger than dead trees. The woodland structure at AW reserve varied from west to east with a higher stand density in the AW1 plot (600 stems ha^{-1}) compared to the AW2 plot (428 stems ha^{-1}); AW1 plot is also characterized by the highest abundance of large trees (16 trees ha^{-1}) within the reserve. However, in both plots living and dead trees had similar DBH distributions. At NP, dead trees were on average 1.5 times larger than live trees and the mean basal area for the four plots was 19 ± 0.9 m^2/ha^{-1} (mean ± SD). The live tree distribution at Napier Park was dominated by trees with a DBH of 0.15 ± 0.17 m with few very large trees (DBH > 0.6 m).

3.2. Water balance

Seasonal patterns of T_a, R_s, and VPD were similar across all study sites during the two year study period (Fig. 3). Compared to the alternate year, mean temperatures were higher during November 2017 and January and February 2018 with the last two months characterized by a large number of very warm nights having temperatures over 25 °C. The environmental factors (R_s and VPD) influencing tree transpiration strengthened from winter to summer, with R_s characterized by monthly means ranging between 4 and 25 MJ m^{-2} and monthly means of VPD varying from 1 to 2.5 kPa. The maximum recorded hourly mean R_s was 1200 W m^{-2} in summer and 520 W m^{-2} during winter for AW and NP, and 910 W m^{-2} in summer to 415 W m^{-2} in winter for ND. The average maximum recorded VPD in an hour ranged from 7.4 kPa (ND), 6.1 (AW), and 5.95 (NP) during summer 2018 to 1.8 kPa (for all sites) during winter 2018; lower values were recorded during summer and winter 2017.

Rainfall (P) did not display a marked seasonal variation, but varied significantly among the study sites for both the 2017 and 2018 water years, decreasing as expected from west to east (Fig. 4a). During the 2017 water year, rainfall was close to the 50-year average with winter and spring above average; the 2018 water year was drier than average, despite the wetter months of December and January (Fig. 4a; Fig. 3).

Observed transpiration (T) at reserve scale (Fig. 3) displayed a distinct seasonal pattern, particularly at ND where higher tree density overall led to higher transpiration rates. Transpiration ranged from 11.5 mm month^{-1} in June 2017 to 40.8 mm month^{-1} in January 2018, with an average of 26.2 mm month^{-1}. Lower transpiration rates were measured in AW where DBH are much lower than ND. Transpiration at AW ranged from 12.2 mm month^{-1} in June 2017 to 22.4 mm month^{-1} in January 2018, with an average of 17.6 mm month^{-1}. Transpiration rates in different months at NP were similar in the two years, with an average transpiration of about 7.5 mm month^{-1}.

Temporal averaged θ (calculated as the mean of all the measurements over the study period in each site) shows different soil moisture profiles in the sites (Fig. 4b). Shallow layers of soil remained relatively dry at AW ($\theta < 0.05\,\text{m}^3\,\text{m}^{-3}$) with a more pronounced response to rainfall events at depths of about 1 m, particularly for the wetter year 2017. Conversely, at ND and NP, θ in shallow layers varied more compared to deeper layers. Three distinct soil zones could be identified at NP: very dry topsoil, increasingly wet layers between 0.3 to 0.6 m, and near-saturated layers below. These profiles clearly reflect the profile of soil texture at the three sites.

Water table depth (Fig. 5) at AW had a visible seasonal cycle with recharge from rainfall occurring between September and December. At ND, groundwater appeared to be less sensitive to rainfall, but conversely the effects of prolonged rain-free periods were more pronounced. In particular, an increase of 0.35 m in the depth to groundwater table was recorded during the 20 days without rain between February and March 2017, and an increase of 0.18 m was measured during the 14-day rain free period in March 2018.

The data of P, T, θ, and water table levels were used to estimate the water balance of the reserves (Table 2), with considerable inter-annual and inter-site variability in the water balance components during the two years (2017–2018). ND received about 789 mm of rain, while for the irrigated site (i.e., NP) the total amount of incoming water including both the annual precipitation and the irrigation water was 100 mm. Despite more rainfall during 2017 than during 2018, the site-averaged transpiration was quite similar for the two years of study. Of this rainfall, about 297–332 mm (42–45% of the annual rainfall) was returned to the atmosphere through tree transpiration at ND, 205-210 mm (31-35%) at AW, and only 85-91 mm (14-18%) at NP, accounting for the high dependency of plot-level transpiration on the number of live trees (Table 1).

Among the three study sites, AW experienced in 2017 a strong soil water depletion in the first 1.2 m of monitored soil (−60 mm) with a pronounced recharge to groundwater (+16 mm). The opposite behavior was recorded in 2018 when a considerable decline of ΔS_{gw} (−31 mm) occurred, while the water content of the unsaturated zone increased. $\Delta S_{sw,s}$ increased overall at ND (+15 mm in 2017 and + 9 mm in 2018), whereas small variations were observed with respect to ΔS_{gw}. Taking into account only $\Delta S_{sw,s}$, NP showed a response similar to AW, with a decline in 2017 and an increase in 2018.

The annual water balance closure, $ET + \Delta S_{sw} + \epsilon$, varied from 351 to 588 mm yr^{-1}, representing 56, 75, and 96% of P during the wet year 2017 and 53, 66, and 88% during the dry year 2018 for ND, AW, and

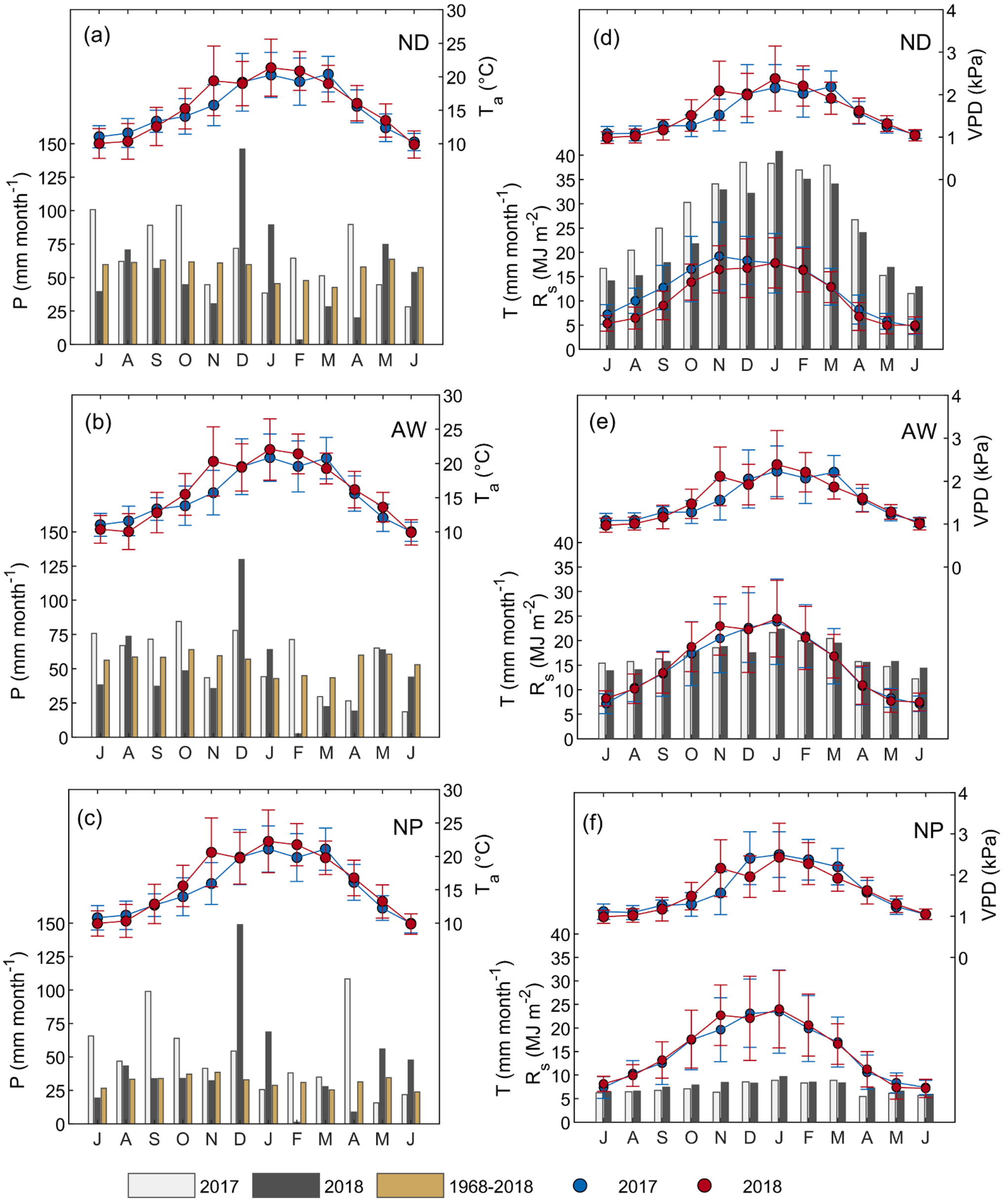

Fig. 3. (a–c) Monthly rainfall (P) (bars) and monthly mean (± SD) of air temperature (T_a) for ND, AW, and NP. (d–f) Monthly transpiration (T) losses (bars) and monthly mean (± SD) of solar radiation (R_s) and vapor pressure deficit (VPD) for ND, AW, and NP.

NP, respectively. These values are further discussed in Section 4.

3.3. Groundwater uptake by vegetation

Diurnal fluctuations in the depth to the groundwater table were observed during several rain-free days for both 2017 and 2018 at ND (Fig. 6a and Fig. 6c). As SFD increased during the daylight hours, the depth to groundwater table declined, while during the night a reduction in tree transpiration coincided with a rise in the water table, indicating a recovery flux toward the bore. These patterns of water table are often associated with groundwater uptake by tree roots for transpiration (Loheide et al., 2005; Orellana et al., 2012).

A total of 8 days were selected within the two prolonged rain-free periods in 2017 and 2018. Using Eq. (4), groundwater uptake (T_{gw}) was estimated to range between 0.4 and 1.1 mm d^{-1}, for a total of 5 mm during the 2017 rain-free period, and between 0.04 and 0.6 mm d^{-1}, for a total of 2.6 mm during the 2018 rain-free period. Therefore, about 42% (SD ± 16%) and 29% (SD ± 15%) of transpiration was estimated to be from groundwater in those periods (Fig. 6b and Fig. 6d).

It was not possible to detect a clear diurnal water table signal at AW. The delay in the downward propagation of air pressure through the pores of the unsaturated zone generated water fluctuations in the bore that overshadowed the diurnal signal. Examining the trends in soil water content (Fig. 4b) and transpiration rates during the prolonged rain-free periods in 2017 and 2018 suggested that transpiration rates were not limited by the modest soil water availability. The diurnal shrinking and swelling of the tree trunk for EV1 along with sustained SFD also supported the presence of T_{gw} at AW (Fig. 7). Swelling started in the late afternoon when the evaporative demand decreased considerably, and continued throughout the night due to the water uptake; as evapotranspiration demand increased during the daylight hours, shrinkage occurred. The contribution of groundwater uptake to the total transpiration was quantified by estimating the change in water table depth attributed to the specific rain-free period. Using this method, a total of 2.8 mm of T_{gw} was estimated for the 8 days between February and March 2017, being about 47% of total transpiration. A

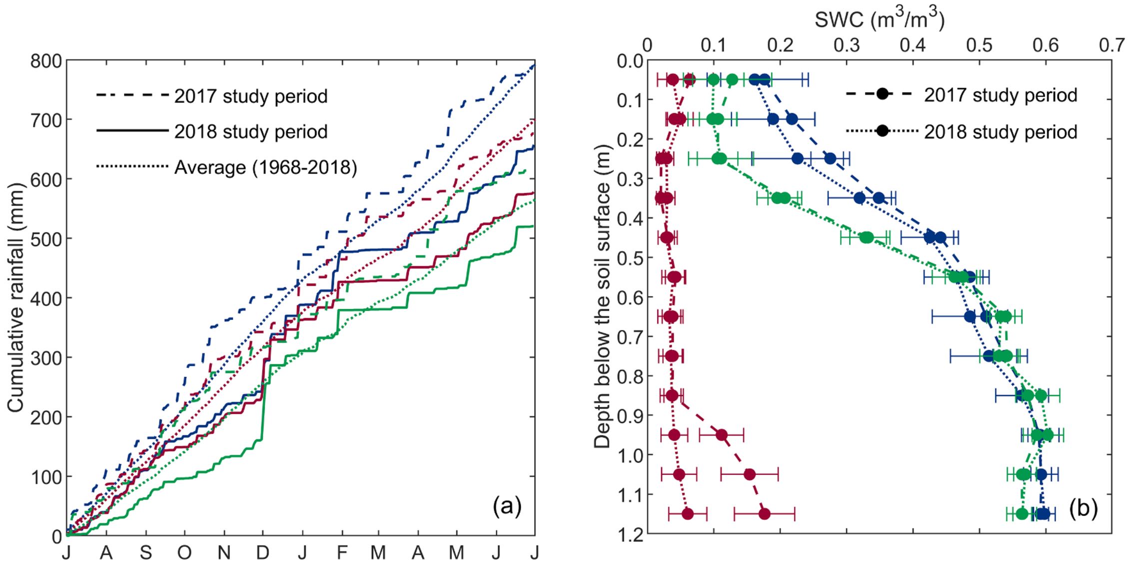

Fig. 4. Comparison of (a) cumulative rainfall during the 2017–2018 study period with the 50-year average (1968–2018) and (b) temporal-averaged soil volumetric water content (θ) in the first 1.2 m of soil profile for: ND (blue), AW (red), and NP (green). (For interpretation of the references to colour in this figure legend, the reader is referred to the web version of this article.)

small data gap did not allow T_{gw} to be estimated for the 2018 summer rain-free period.

3.4. *Night-time tree water use*

Warm summer nights with temperatures above 25°C following days with temperatures above 35°C occurred a few times within the two years of this study. In most circumstances, trees under observation coped well with these short heat events and did not lose their hydraulic functions. Substantial night-time SFD was recorded in both EV1 and EV3 during the nights between 7 and 8 of January and between 8 and 9 of February 2017 (Fig. 8a and Fig. 8d). The high temperatures on these nights were associated with consequent high VPD, which likely led to transpiration during the night. During the two recorded warm summer nights SFD_n was found to be about 11% (EV1) and 16% (EV3) of the daily water use for January 2017, and about 3% (EV1) and 13% (EV3) for February 2017.

Measurements of diurnal shrinking and swelling of the tree trunk also verified the presence of night-time water use. During the first warm night, swelling, usually occurring near sunset when the evaporative demand decreased, coincided with a reduced amplitude due to the

Table 2
Water balance components on an annual (water year) basis[a].

Study Sites	ID	WY	P	Irr	T	$\Delta S_{sw,s}$	ΔS_{gw}	$ET + \Delta S_{sw,d} + \epsilon$[b]
National Drive	ND	2017	789	0	332	15	2	441
		2018	657	0	297	9	− 1	351
Alex Wilkie	AW	2017	676	0	210	− 60	16	510
		2018	578	0	205	20	− 31	384
Napier Park	NP	2017	615	50	85	− 8	n/a	588
		2018	520	50	91	23	n/a	456

[a] WY: Water Year (1 July to 30 June); P: Rainfall; Irr: Imported water (i.e., irrigation); T: Tree transpiration; $\Delta S_{sw,s}$: Change in soil water storage in the first 1.2 m of monitored soil; $\Delta S_{sw,d}$: Change in soil water storage in the deep soil (below 1.2 m); ΔS_{gw}: Change in groundwater water storage; ET: evapotranspiration ($ET = ET_{floor} + E_i$) which includes floor evapotranspiration (ET_{floor}), including grass, ferns, and small shrubs, as well as soil evaporation, and canopy interception (E_i); ϵ: Water balance errors; n/a: data not available. All water variables are in mm yr^{-1}.

[b] Surface runoff (Q) negligible in all sites.

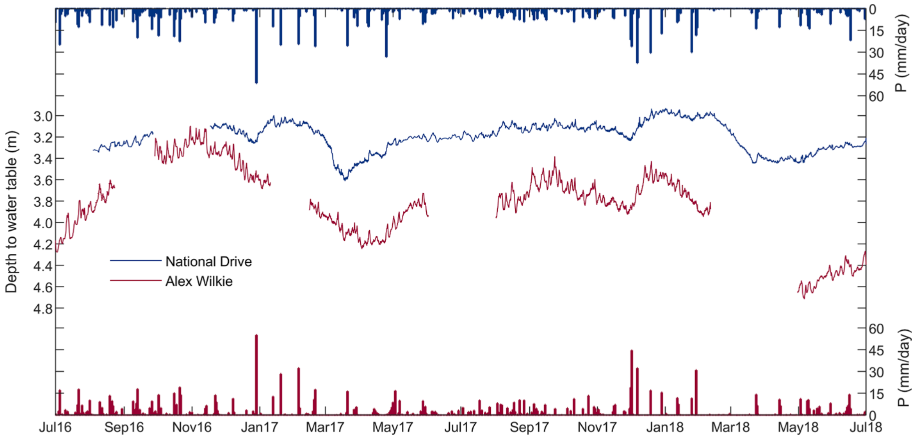

Fig. 5. Dynamics of rainfall events and depth to water table observed at ND and AW during the study period (groundwater was not monitored at NP).

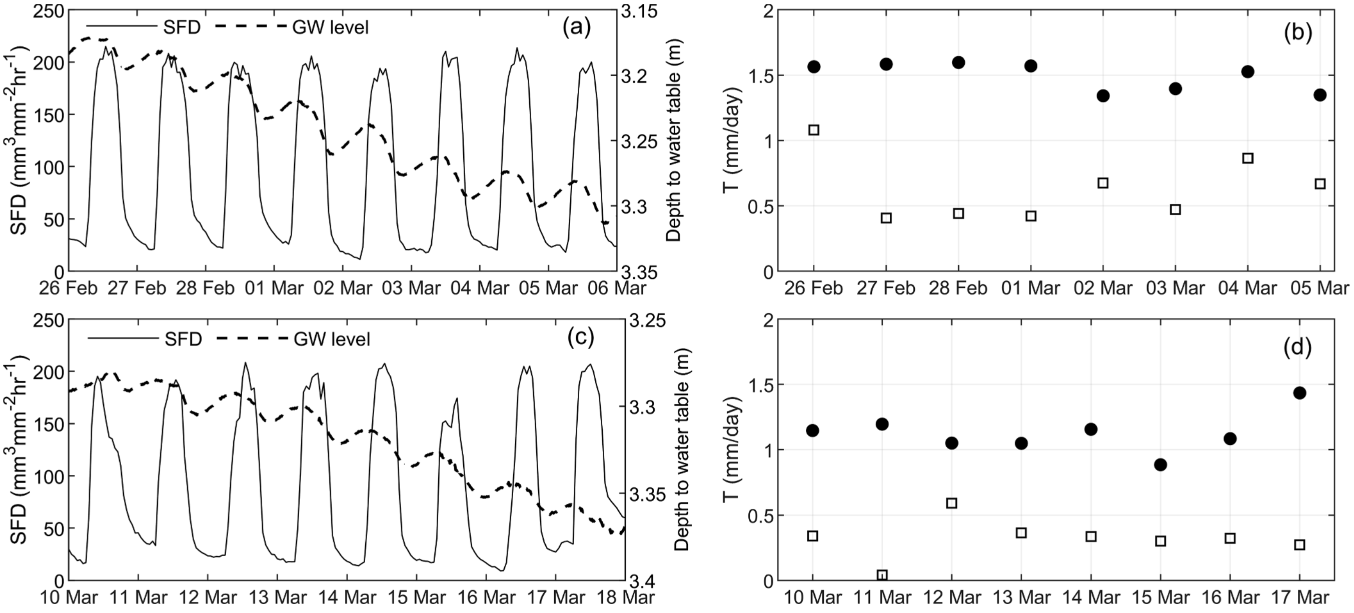

Fig. 6. Diurnal groundwater fluctuations and sap flux density (SFD) for a selection of 8 rain-free days for the (a) 2017 and (c) 2018 water years at ND. Daily groundwater uptake from the fluctuation method (T_{gw}) (open square) and transpiration fluxes (solid circle) for the 8 days rain-free period of the (b) 2017 and (d) 2018 water years at ND.

night-time transpiration, causing an even larger shrinkage when the evaporative demand increased during the following daylight hours (Fig. 8b and Fig. 8c). This phenomenon was also present during the second warm night even though recent rainfall events affected the diurnal signal of DBH (Fig. 8e and Fig. 8f).

4. Discussion

This study attempts to understand and quantify the water balance and tree water use of small urban reserves. In two of the study sites (i.e., ND and AW) groundwater was found to play an essential role in supporting tree transpiration, especially during the driest periods of the year and heat events. At NP, groundwater not being easily accessible, the water stored in the shallow clay layer of the duplex soil supported transpiration rates, as observed in other similar conditions (Verma et al., 2014).

Observed transpirations rates were found to be comparable to estimates from other *Eucalyptus* stands in natural areas (e.g., Zeppel et al., 2006; Doody et al., 2015). Transpiration rates at ND ranged from 1.3 to 0.5 mm day^{-1} during summer and winter, while at AW they were from 0.9 to 0.25 mm day^{-1}; at NP, T ranged between 0.3 mm day^{-1} during summer and 0.1 mm day^{-1} in winter. In both years, T was about 44% (ND), 33% (AW), and 16% (NP) of total annual rainfall, showing large inter-site variability due to different natural rainfall regimes and stand density (Table Table 1; Table 2); on the contrary, small inter-annual variability was observed, although annual rainfall in 2018 was about 15% lower than 2017.

In both years, a large portion of the water balance closure was

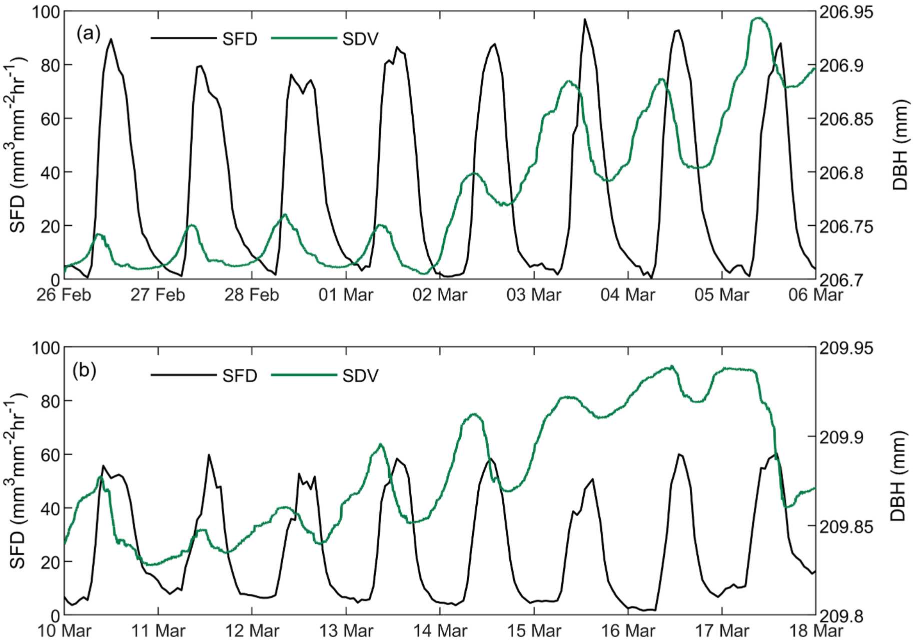

Fig. 7. Sap flux density (SFD) and DBH for a selection of 8 rain-free days for the (a) 2017 and (b) 2018 water years at AW.

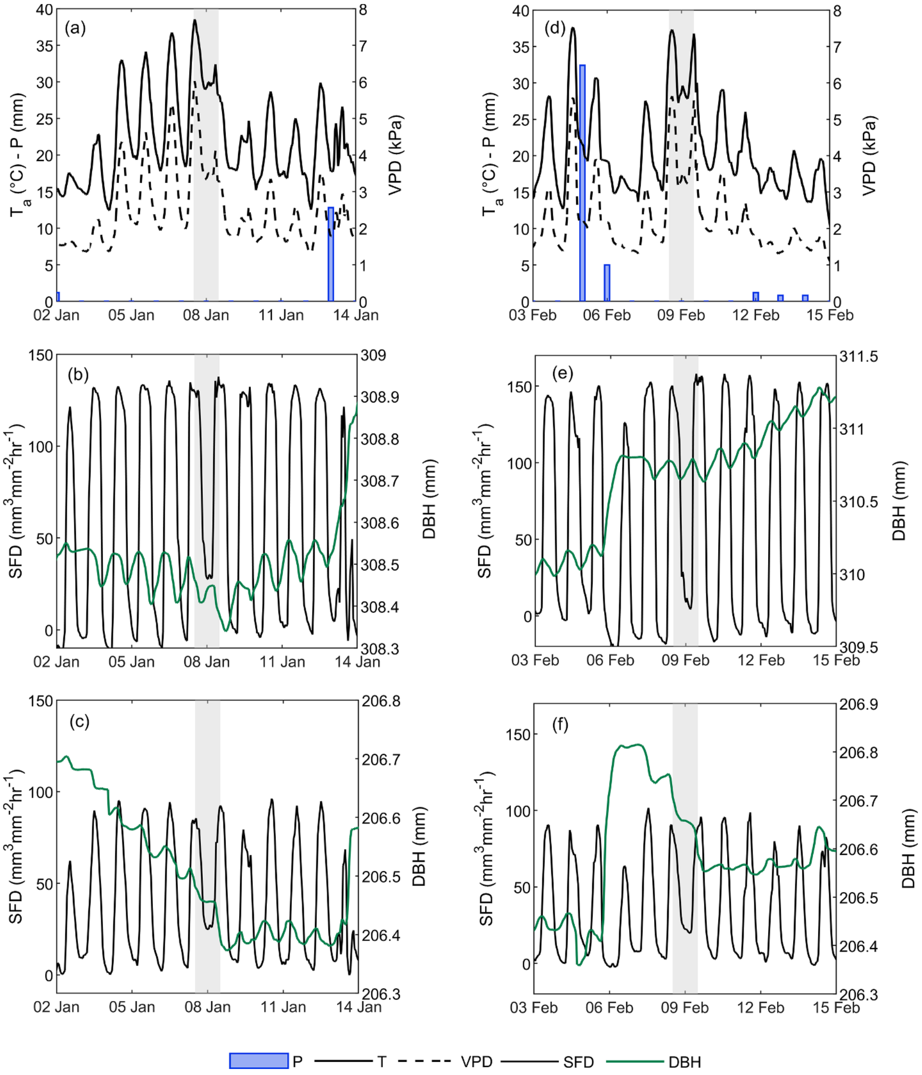

Fig. 8. Time evolution of environmental factors, sap flux density (SFD), and DBH during the night-time heat stress events observed in January and February 2017 at AW: (a, d) air temperature (T_a), vapor pressure deficit (VPD), and rainfall (P); (b, e) SFD and DBH for the EV1 tree; and (c, f) SFD and DBH for the EV3 tree.

attributed to ET (i.e., ET_{floor} + E_i) and $\Delta S_{sw,d}$. The magnitude of ET and $\Delta S_{sw,d}$ can be estimated from previous studies conducted on similar vegetation cover and hydrologic regime (Benyon and Doody, 2015).

Specifically, ET_{floor} may represent more than 50% of total ET (Zeppel et al., 2006) and about 23-37% of the annual rainfall (Benyon and Doody, 2015), whereas E_i may be between 15 to 26% of the total annual rainfall (Dunin et al., 1988; Farrington and Bartle, 1991; Hutley et al., 2000; Bulcock and Jewitt, 2012). Accordingly, considering ET_{floor} + E_i about 50% of the annual rainfall, this term accounted for 89% (ND), 66% (AW), and 52% (NP) of the water balance closure for the 2017 water year, and 94% (ND), 75% (AW), and 57% (NP) for the 2018 water year.

These estimates support the water balance in Table 2, especially for ND, in which $\Delta S_{sw,d}$ is expected to be small due to the clayey nature of the soil, which enhances the capillary rise up to the monitored soil layers (as also shown in Fig. 4b). At AW, higher proportions of interception losses (E_i) should be considered due to the dense understory cover. As well, higher $\Delta S_{sw,d}$ may be expected because of the highly sandy soil which increases the movement of water beyond the monitored soil profile. At NP the water balance was only conducted for the monitored soil (0 - 1.2 m), with $\Delta S_{sw,d}$ representing the downward drainage below this depth; at this site, extensive grassy and bare soil areas may also contribute to a larger percentage of floor evaporation.

Most of the uncertainties in the estimates of the water balance components are related to the underestimation of canopy transpiration. Accounting for an underestimation of T of 35% would result in an annual water balance closure of 41, 65, and 91% of P during 2017 and 38, 54, and 81% in 2018 for ND, AW, and NP, respectively. This may involve, in particular at ND, a different water balance closure partitioning with less water lost through ET_{floor}.

Groundwater use by vegetation at the ND and AW reserves illustrates the important role that groundwater resources may have in supporting tree transpiration in urban areas, where arduous growing conditions and abiotic stress factors, such as heat stress and low moisture conditions, affect the health of trees. Several studies have detected similar behaviors, but commonly with reference to large biodiverse ecosystems and often in natural environments or environments mildly affected by human activities (e.g., Fan et al., 2014; Fan et al., 2016; Balugani et al., 2017). In this study, groundwater transpiration (T_{gw}) was estimated to contribute about 30–40% of total T in the driest period of the year; this is consistent with the findings from other studies, showing that groundwater was a source of water for vegetation (Orellana et al., 2012). The annual value of T_{gw} is difficult to estimate precisely because of the assumptions in the definition of Eq. (4). The difficulties in the estimation of S_y (Gehman et al., 2009; Dietrich et al., 2018) and the lack of information on the groundwater flows in and out of the reserves introduce uncertainties in the estimation of T_{gw} (Loheide et al., 2005). However, the water table patterns during dry periods and the sustained transpiration rates during and following warm nights strongly support the assumption that trees are using groundwater at ND and AW.

As shown in Drake et al. (2018), water availability played an essential role during heat events. During the study period, the monitored trees successfully coped with warm summer nights with temperatures above 25°C and did not lose their hydraulic functions. In particular, T_n ranged from 3 to 16% of the daily transpiration, which is comparable to those found in eucalyptus woodland in Western Australia (~15–20%) (Dawson et al., 2007) and in New South Wales (~6–8% and up to 19% on some days) (Zeppel et al., 2010; Fan et al., 2016).

5. Conclusion

Urbanization and the associated land use changes greatly impact natural ecosystems, causing small natural reserves in urban areas to face changes in their hydrologic regime. This study provides a comprehensive analysis of the water balance and tree water use dynamics over a two-year period in three urban reserves hosting remnant native vegetation and experiencing different rainfall patterns in Melbourne, Australia. The water balances (2017–2018) showed that the three urban reserves had enough water to sustain transpiration rates despite the urban surrounding. Two of the reserves of this study appeared to be dependent on groundwater and the other one relied on water stored in a clay layer of its duplex soil. Groundwater played an essential role in sustaining transpiration rates. During the driest periods of the year, transpiration from groundwater was estimated to be about 30-40 % of the total transpiration. During warm nights following days with temperatures above 35 °C, groundwater allows trees to transpire between 3 and 16% of the total daily transpiration. Therefore, these results highlight the importance of soil water resources in urban areas to support green spaces.

In future studies, more attention should be given to quantify groundwater dynamics in urban areas, to understand how changes in water table due to urbanization and climate variations may impact groundwater dependent vegetation. A quantification of groundwater fluxes to and from the reserves would helped better constrain the transpiration from the understorey (i.e., ET_{floor}). Longer series of sap flow measurements and tree diameter variations would also support a better understanding of how trees respond to different forms of stress.

Understanding the water requirements of urban reserves may assist government authorities in improving management effectiveness for these ecosystems through measures such as irrigation.

Declaration of Competing Interest

None.

Acknowledgments

The study was supported by the Australian Research Council, and the City of Greater Dandenong and Mooney Valley City councils through the Linkage project LP150100901. The authors thankfully acknowledge the help from K. Mason, P. Fisher, B. Salmi, A. Moodie, M. Keenan, M. Gooding, G. Horner, M. McGeoch, G.A. Oppedisano, and M. McClymont for data collection.

References

Asawa, T., Kiyono, T., Hoyano, A., 2017. Continuous measurement of whole-tree water balance for studying urban tree transpiration. Hydrol. Process. 31, 3056–3068.

Balugani, E., Lubczynski, M., Reyes-Acosta, L., Van Der Tol, C., Francés, A., Metselaar, K., 2017. Groundwater and unsaturated zone evaporation and transpiration in a semi-arid open woodland. J. Hydrol. 547, 54–66.

Barron, O., Barr, A., Donn, M., 2013. Effect of urbanisation on the water balance of a catchment with shallow groundwater. J. Hydrol. 485, 162–176.

Benyon, R., Doody, T., 2015. Comparison of interception, forest floor evaporation and transpiration in Pinus radiata and Eucalyptus globulus plantations. Hydrol. Process. 29, 1173–1187.

Berland, A., Shiflett, S.A., Shuster, W.D., Garmestani, A.S., Goddard, H.C., Herrmann, D.L., Hopton, M.E., 2017. The role of trees in urban stormwater management. Landscape Urban Plann. 162, 167–177.

Bowler, D.E., Buyung-Ali, L., Knight, T.M., Pullin, A.S., 2010. Urban greening to cool towns and cities: a systematic review of the empirical evidence. Landscape Urban Plann. 97, 147–155.

Bradshaw, C.J., 2012. Little left to lose: deforestation and forest degradation in Australia since European colonization. J. Plant Ecol. 5, 109–120.

Bulcock, H., Jewitt, G., 2012. Field data collection and analysis of canopy and litter interception in commercial forest plantations in the KwaZulu-Natal Midlands, South Africa. Hydrol. Earth Syst. Sci. 16, 3717–3728.

Burgess, S.S., Adams, M.A., Turner, N.C., Beverly, C.R., Ong, C.K., Khan, A.A., Bleby, T.M., 2001. An improved heat pulse method to measure low and reverse rates of sap flow in woody plants. Tree Physiol. 21, 589–598.

Chen, L., Zhang, Z., Li, Z., Tang, J., Caldwell, P., Zhang, W., 2011. Biophysical control of whole tree transpiration under an urban environment in Northern China. J. Hydrol. 402, 388–400.

Dawson, T.E., Burgess, S.S., Tu, K.P., Oliveira, R.S., Santiago, L.S., Fisher, J.B., Simonin, K.A., Ambrose, A.R., 2007. Nighttime transpiration in woody plants from contrasting ecosystems. Tree Physiol. 27, 561–575.

Declet-Barreto, J., Knowlton, K., Jenerette, G.D., Buyantuev, A., 2016. Effects of urban vegetation on mitigating exposure of vulnerable populations to excessive heat in Cleveland, Ohio. Weather Clim. Soc. 8, 507–524.

DELWP, 2016. Victoria in future 2016. The State of Victoria Department of Environment, Land, Water and Planning.

Dietrich, S., Carrera, J., Weinzettel, P., Sierra, L., 2018. Estimation of specific yield and its variability by electrical resistivity tomography. Water Resour. Res. 54, 8653–8673.

van Dijk, A.I., Beck, H.E., Crosbie, R.S., de Jeu, R.A., Liu, Y.Y., Podger, G.M., Timbal, B., Viney, N.R., 2013. The Millennium Drought in southeast Australia (2001–2009): natural and human causes and implications for water resources, ecosystems, economy, and society. Water Resour. Res. 49, 1040–1057.

Doody, T.M., Colloff, M.J., Davies, M., Koul, V., Benyon, R.G., Nagler, P.L., 2015. Quantifying water requirements of riparian river red gum (Eucalyptus camaldulensis) in the Murray-Darling Basin, Australia–implications for the management of environmental flows. Ecohydrology 8, 1471–1487.

Drake, J.E., Tjoelker, M.G., Vårhammar, A., Medlyn, B.E., Reich, P.B., Leigh, A., Pfautsch, S., Blackman, C.J., López, R., Aspinwall, M.J., et al., 2018. Trees tolerate an extreme heatwave via sustained transpirational cooling and increased leaf thermal tolerance. Glob. Change Biol. 24, 2390–2402.

Dunin, F., O'loughlin, E., Reyenga, W., 1988. Interception loss from eucalypt forest: lysimeter determination of hourly rates for long term evaluation. Hydrol. Process. 2, 315–329.

Eamus, D., Froend, R., 2006. Groundwater-dependent ecosystems: the where, what and why of GDEs. Aust. J. Bot. 54, 91–96.

Elmqvist, T., Setälä, H., Handel, S., Van Der Ploeg, S., Aronson, J., Blignaut, J.N., Gomez-Baggethun, E., Nowak, D., Kronenberg, J., De Groot, R., 2015. Benefits of restoring ecosystem services in urban areas. Curr. Opin. Environ. Sustain. 14, 101–108.

Endter-Wada, J., Kurtzman, J., Keenan, S.P., Kjelgren, R.K., Neale, C.M., 2008. Situational waste in landscape watering: residential and business water use in an urban utah community 1. J. Am. Water Resour. Assoc. 44, 902–920.

Fan, J., Oestergaard, K.T., Guyot, A., Lockington, D.A., 2014. Estimating groundwater recharge and evapotranspiration from water table fluctuations under three vegetation covers in a coastal sandy aquifer of subtropical Australia. J. Hydrol. 519, 1120–1129.

Fan, J., Ostergaard, K.T., Guyot, A., Fujiwara, S., Lockington, D.A., 2016. Estimating groundwater evapotranspiration by a subtropical pine plantation using diurnal water table fluctuations: Implications from night-time water use. J. Hydrol. 542, 679–685.

Farrington, P., Bartle, G., 1991. Recharge beneath a Banksia woodland and a Pinus pinaster plantation on coastal deep sands in south Western Australia. For. Ecol. Manage. 40, 101–118.

Forster, M.A., 2014. How significant is nocturnal sap flow? Tree Physiol. 34, 757–765.

Gehman, C.L., Harry, D.L., Sanford, W.E., Stednick, J.D., Beckman, N.A., 2009. Estimating specific yield and storage change in an unconfined aquifer using temporal gravity surveys. Water Resour. Res. 45.

Gill, S.E., Handley, J.F., Ennos, A.R., Pauleit, S., 2007. Adapting cities for climate change: the role of the green infrastructure. Built Environ. 33, 115–133.

Hahs, A.K., McDonnell, M.J., 2014. Extinction debt of cities and ways to minimise their realisation: a focus on Melbourne. Ecol. Manage. Restoration 15, 102–110.

Hutley, L., O'Grady, A., Eamus, D., 2000. Evapotranspiration from Eucalypt open-forest savanna of Northern Australia. Funct. Ecol. 14, 183–194.

Johnson, A.I., 1963. Compilation of specific yield for various materials. Technical Report. USGS Numbered Series.

Lepczyk, C.A., Aronson, M.F., Evans, K.L., Goddard, M.A., Lerman, S.B., MacIvor, J.S., 2017. Biodiversity in the city: fundamental questions for understanding the ecology of urban green spaces for biodiversity conservation. Bioscience 67, 799–807.

Litvak, E., Manago, K., Hogue, T., Pataki, D., 2017. Evapotranspiration of urban landscapes in Los Angeles, California at the municipal scale. Water Resour. Res. 53, 4236–4252.

Litvak, E., McCarthy, H.R., Pataki, D.E., 2011. Water relations of coast redwood planted in the semi-arid climate of southern California. Plant Cell Environ. 34, 1384–1400.

Litvak, E., Pataki, D.E., 2016. Evapotranspiration of urban lawns in a semi-arid environment: an in-situ evaluation of microclimatic conditions and watering recommendations. J. Arid Environ. 134, 87–96.

Livesley, S., McPherson, E., Calfapietra, C., 2016. The urban forest and ecosystem services: impacts on urban water, heat, and pollution cycles at the tree, street, and city scale. J. Environ. Qual. 45, 119–124.

Loheide, S.P., Butler Jr, J.J., Gorelick, S.M., 2005. Estimation of groundwater consumption by phreatophytes using diurnal water table fluctuations: a saturated-unsaturated flow assessment. Water Resour. Res. 41.

Matheny, A.M., Bohrer, G., Garrity, S.R., Morin, T.H., Howard, C.J., Vogel, C.S., 2015. Observations of stem water storage in trees of opposing hydraulic strategies. Ecosphere 6, 1–13.

McCarthy, H.R., Pataki, D.E., 2010. Drivers of variability in water use of native and non-native urban trees in the greater Los Angeles area. Urban Ecosyst. 13, 393–414.

McKinney, M.L., 2002. Urbanization, Biodiversity, and Conservation: the impacts of urbanization on native species are poorly studied, but educating a highly urbanized human population about these impacts can greatly improve species conservation in all ecosystems. Bioscience 52, 883–890.

Meinzer, F.C., James, S.A., Goldstein, G., 2004. Dynamics of transpiration, sap flow and use of stored water in tropical forest canopy trees. Tree Physiol. 24, 901–909.

Melaas, E.K., Wang, J.A., Miller, D.L., Friedl, M.A., 2016. Interactions between urban vegetation and surface urban heat islands: a case study in the Boston metropolitan region. Environ. Res. Lett. 11, 054020.

Nadezhdina, N., Čermák, J., Ceulemans, R., 2002. Radial patterns of sap flow in woody stems of dominant and understory species: scaling errors associated with positioning of sensors. Tree Physiol. 22, 907–918.

O'Grady, A., Cook, P., Howe, P., Werren, G., 2006. Groundwater use by dominant tree species in tropical remnant vegetation communities. Aust. J. Bot. 54, 155–171.

O'Kelly, B.C., 2004. Accurate determination of moisture content of organic soils using the oven drying method. Drying Technol. 22, 1767–1776.

Orellana, F., Verma, P., Loheide, S.P., Daly, E., 2012. Monitoring and modeling water-vegetation interactions in groundwater-dependent ecosystems. Rev. Geophys. 50.

Pataki, D., Boone, C., Hogue, T., Jenerette, G., McFadden, J., Pincetl, S., 2011. Socio-ecohydrology and the urban water challenge. Ecohydrology 4, 341–347.

Peters, R.L., Fonti, P., Frank, D.C., Poyatos, R., Pappas, C., Kahmen, A., Carraro, V., Prendin, A.L., Schneider, L., Baltzer, J.L., et al., 2018. Quantification of uncertainties in conifer sap flow measured with the thermal dissipation method. New Phytol.

Roberts, B.R., 1977. The response of urban trees to abiotic stress [moisture, temperature, light, pesticides]. J. Arboriculture (USA).

Seto, K.C., Güneralp, B., Hutyra, L.R., 2012. Global forecasts of urban expansion to 2030 and direct impacts on biodiversity and carbon pools. Proc. Natl. Acad. Sci. 109, 16083–16088.

Shields, C., Tague, C., 2015. Ecohydrology in semiarid urban ecosystems: modeling the relationship between connected impervious area and ecosystem productivity. Water Resour. Res. 51, 302–319.

Sieghardt, M., Mursch-Radlgruber, E., Paoletti, E., Couenberg, E., Dimitrakopoulus, A., Rego, F., Hatzistathis, A., Randrup, T.B., 2005. The abiotic urban environment: impact of urban growing conditions on urban vegetation. In: Urban Forests and Trees. Springer, pp. 281–323.

Steppe, K., De Pauw, D.J., Doody, T.M., Teskey, R.O., 2010. A comparison of sap flux density using thermal dissipation, heat pulse velocity and heat field deformation methods. Agric. For. Meteorol. 150, 1046–1056.

Tulloch, A.I., Barnes, M.D., Ringma, J., Fuller, R.A., Watson, J.E., 2016. Understanding the importance of small patches of habitat for conservation. J. Appl. Ecol. 53, 418–429.

Van Loon, A.F., Gleeson, T., Clark, J., Van Dijk, A.I., Stahl, K., Hannaford, J., Di Baldassarre, G., Teuling, A.J., Tallaksen, L.M., Uijlenhoet, R., Hannah, D.M., Sheffield, J., Svoboda, M., Verbeiren, B., Wagener, T., Rangecroft, S., Wanders, N., Van Lanen, H.A.J., 2016. Drought in the anthropocene. Nat. Geosci. 9, 89.

Vandegehuchte, M.W., Guyot, A., Hubeau, M., De Groote, S.R., De Baerdemaeker, N.J., Hayes, M., Welti, N., Lovelock, C.E., Lockington, D.A., Steppe, K., 2014. Long-term versus daily stem diameter variation in co-occurring mangrove species: environmental versus ecophysiological drivers. Agric. For. Meteorol. 192, 51–58.

Verma, P., Loheide II, S.P., Eamus, D., Daly, E., 2014. Root water compensation sustains transpiration rates in an australian woodland. Adv. Water Resour. 74, 91–101.

White, W.N., 1932. A method of estimating ground-water supplies based on discharge by plants and evaporation from soil: results of investigations in Escalante Valley, Utah, volume 659 US Government Printing Office.

Xiao, Q., McPherson, E., Simpson, J., Ustin, S., 2007. Hydrologic processes at the urban residential scale. Hydrol. Process. 21, 2174–2188.

Yang, Y., Endreny, T.A., Nowak, D.J., 2015. Simulating the effect of flow path roughness to examine how green infrastructure restores urban runoff timing and magnitude. Urban For. Urban Green. 14, 361–367.

Zeppel, M., Tissue, D., Taylor, D., Macinnis-Ng, C., Eamus, D., 2010. Rates of nocturnal transpiration in two evergreen temperate woodland species with differing water-use strategies. Tree Physiol. 30, 988–1000.

Zeppel, M.J., Yunusa, I.A., Eamus, D., 2006. Daily, seasonal and annual patterns of transpiration from a stand of remnant vegetation dominated by a coniferous callitris species and a broad-leaved eucalyptus species. Physiol. Plant. 127, 413–422.

Zipper, S.C., Schatz, J., Kucharik, C.J., Loheide, S.P., 2017. Urban heat island-induced increases in evapotranspirative demand. Geophys. Res. Lett. 44, 873–881.